Article

Detailed Mechanistic Study of the Non-enzymatic Formation of the Discoipyrrole Family of Natural Products

Dominic A. Colosimo, and John B. MacMillan

J. Am. Chem. Soc., **Just Accepted Manuscript** • DOI: 10.1021/jacs.5b13320 • Publication Date (Web): 29 Jan 2016

Detailed Mechanistic Study of the Non-enzymatic Formation of the Discoipyrrole Family of Natural Products

Dominic A. Colosimo and John B. MacMillan*

Department of Biochemistry, University of Texas Southwestern Medical Center. 5323 Harry Hines Blvd, Dallas, TX USA 75390

ABSTRACT: The discoipyrroles A-D (DPA-DPD) are recently discovered natural products produced by the marine bacteria, *Bacillus hunanensis,* which exhibit anti-cancer properties *in-vitro*. Initial biosynthetic studies demonstrated that DPA was formed in the liquid fermentation media of *B. hunanensis* from three secreted metabolites through an unknown, but protein independent mechanism. The increased identification of natural products who depend on non-enzymatic steps create a significant need to understand how these different reactions can occur. Here, we utilized ^{15}N labeled starting materials and continuous high-sensitivity ^{1}H-^{15}N HMBC NMR to resolve scarce reaction intermediates of the non-enzymatic discoipyrrole reaction as they formed in real time. This information guided supplemental experiments, using ^{13}C and ^{18}O labeled materials, to elucidate the details of discoipyrrole A's non-enzymatic biosynthesis which features a highly concerted pyrrole formation and necessary O_2 mediated oxidation. We have illustrated a novel way of using isotopically enhanced two-dimensional NMR to interrogate reaction mechanisms as they occur. In addition, these findings added to our growing knowledge of how multi-component non-enzymatic reactions can occur through inherently reactive bacterial metabolites.

INTRODUCTION

The discoipyrroles (DPs) are a family of natural products that were isolated from the bacterial fermentation of *Bacillus hunanensis* strain SNA-048. The DPs were shown to be inhibitors of discoidin domain receptor-2 (DDR2) dependent cell migration of BR5 human foreskin fibroblasts and potent cytotoxins to DDR2 mutant non-small cell lung cancer cell lines[1].

In the initial report of DPA (**1**) we demonstrated its production in the aqueous fermentation media of *SNA-048* via a protein independent multi-component reaction from three starting materials; 4-hydroxysattabacin (**4**), anthranilic acid (**5**), 4-hydroxybenzaldehyde (**6**). The non-enzymatic nature of this reaction was demonstrated through a series of feeding studies in fermentation media depleted of bacteria and proteins via filtration and heating, respectively. We were further able to recapitulate the chemistry in organic solvent via a three-step procedure that was later utilized towards the total synthesis of discoipyrrole D (**3**) reported by the May laboratory[2].

It is well established that bacteria most often use complimentary enzymes to sequentially catalyze bond formation in natural product biosynthesis, and that these proteins are expressed from highly conserved and organized clusters of genes [3]. However, there have been increasing number of cases where isolated secondary metabolites differ from their predicted structure due to non-enzymatic reactions stemming from serendipitous proximity of complimentary reactive metabolites[4]. The knowledge gained from interrogating these mechanisms has fueled inventive and effective techniques to generate analogs with improved biological activities[5].

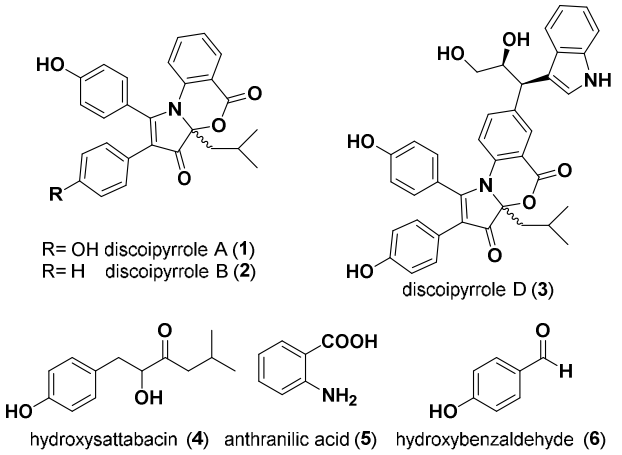

Figure 1. Metabolites found in the fermentation media of *B. hunanensis* strain SNA-048.

Previously described microbial natural products that utilize a non-enzymatic step feature attack of an electrophilic sp^2 carbon of a late-stage enzymatic intermediate by a nucleophile[5-6]. In the case of **1** however, the self-assembly of **4**, **5**, and **6** requires the formation of four covalent bonds as well as two oxidations. Deciphering the mechanism by which the discoipyrroles are formed will expand our general knowledge 0f the types of non-enzymatic reactions to be expected in the milieu of microbial fermentation.

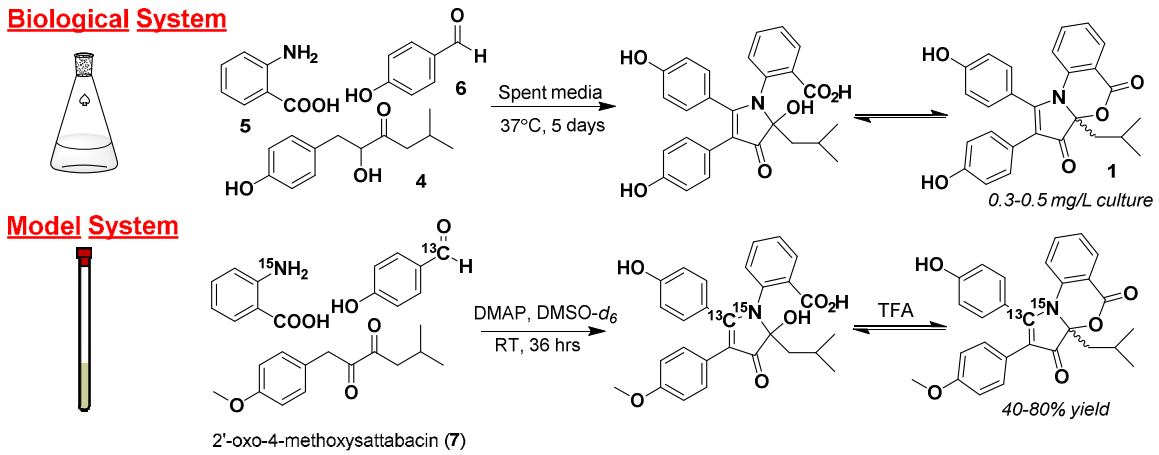

Figure 2. Initial studies of formation of DPA in the fermentation flask were unsuccessful due to low reagent yields, interfering media components, and complicated analytical sample preparation. To combat these issues, precursors were combined in deuterated organic solvent and observed constantly by NMR. The base 4-(dimethylamino)pyridine (DMAP) was used to simulate the basic environment of the fermentation flask (pH = ~9). The oxidation of the acyloin of 4-hydroxysattabacin to form a diketone was known to be a rate limiting step in DPA formation, thus the diketone was prepared with Dess-Martin periodinane (DMP) beforehand to increase the efficiency of the model system.

This understanding will improve our ability to predict natural products that may undergo these reactions. Specific to the discoipyrroles, further understanding of the mechanism of formation can aid in our medicinal chemistry efforts.

RESULTS AND DISCUSSION

Herein we report the details of the non-enzymatic discoipyrrole formation obtained by a combination of NMR and MS approaches utilizing isotopically labeled substrates (^{13}C, ^{15}N, and ^{18}O). In particular, ^{15}N labeled substrates were used for highly sensitive NMR experiments to identify ^{1}H-^{15}N heteronuclear correlations of key intermediates. The increased sensitivity of the isotope label allowed for short (~30 minute) experiments capable of detecting low abundance intermediates in complicated mixtures. This approach could be applied to the study of mechanisms of heteronuclear bond forming reactions, most notably applied to multi-component reactions.

We began our studies of the discoipyrrole formation by examining the origins of the precursor molecules **4**, **5**, and **6**. **4** resembles members of a growing family of acyloin-containing molecules that are products of condensation between two amino acids. **5** and **6** are known degradation products of tryptophan and tyrosine, respectively (KEGG Compounds C00108 and C00633)[7].

To confirm the amino acid origins of **4,** we utilized sequences of known TPP-dependent acyloin synthases to discover homologous candidate genes in the annotated genome of *Bacillus hunanensis* strain *SNA-048* (SI Figure 3)[8]. Particularly of use were the recent findings by Park et al. describing the sattabacin producing acyloin synthase known as Thzk1050 from *Thermosporothrix hazakensis* [8a]. Based on the presence of these putative biosynthetic genes in *SNA-048*, we performed feeding studies with ^{13}C isotope-labeled [2-^{13}C]-L-tyrosine and [2-^{13}C]-L-leucine and confirmed their incorporation into **4** (SI Figure 4). Additional feeding studies and/or genetic analyses were performed to conclude the amino acid sources of **4**, **5**, and **6**. These experiments are described in detail in the supplemental information (SI Text and SI Figures 1-5).

To investigate the non-enzymatic multi-component formation of the discoipyrrole scaffold we took advantage of our previously established synthetic model reaction system in organic solvent. This model takes advantage of starting with the oxidized 4-methoxysattabacin (**7**) (Figure 2), the formation of which we have previously found to be the rate-limiting step in both the fermentation media and organic solvent. Additionally, the model system removes analytical barriers associated with the complex fermentation media. Past successes using NMR active isotope labels for studying reactions through use of kinetic isotopes[9], to elucidate biosynthetic pathways[10], and in the identification of natural products[11] led us to utilize ^{13}C and ^{15}N labeled substrates to probe the multi-component reaction by NMR and MS.

To track the formation of reaction intermediates, the chemical shifts and heteronuclear correlations of key carbon and nitrogen atoms around the pyrrole core were observed in real time. Utilizing [1-^{13}C]-*p*-hydroxybenzaldehyde and ^{15}N-anthranilic acid allowed for observation of heteronuclear NMR correlations from these isotope labels during each of the key bond forming steps. All of the following experiments, unless otherwise noted, were run using 1.0 equivalent of **7**, 2.0 equivalents of **5** and **6** along with 3 equivalents of DMAP. The reactions were carried out in DMSO. For the reactions run in an NMR tube, they were run in a total volume of 700 µL in DMSO-*d6*.

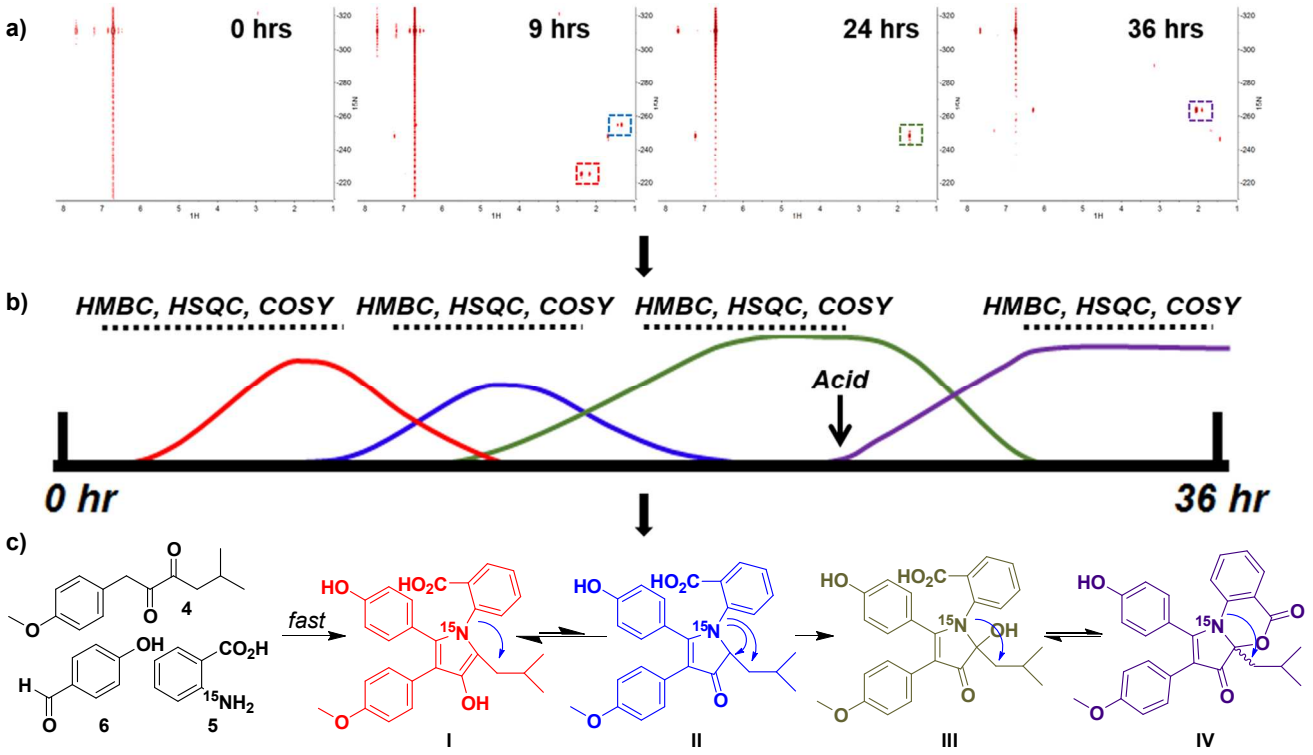

Figure 3. Reaction time course monitored by ^{1}H-^{15}N NMR a) Representative time points from ^{1}H-^{15}N HMBC experiments. Major correlations have been highlighted using colored boxes on the spectra. b) Construction of reaction timeline from ^{1}H-^{15}N HMBC experiments allows for design of additional NMR experiments to elucidate structures of intermediates. c) Structures of intermediates determined through use of 1 and 2D NMR data.

Experimentally we began by carrying out the multi-component reaction with ^{15}N-anthranilic acid and conducted continuous reaction monitoring in 30 minute intervals for 36 hours using ^{1}H-^{15}N HMBC. This methodology provided evidence of C-N bond formation through developing ^{1}H-^{15}N correlations, specifically to downfield ^{1}H signals of the isobutyl chain of **7**. Due to the spectral range of ^{15}N NMR, the ^{15}N chemical shift of anthranilate-derived intermediates provides key structural information on the nature of the C-N bond of an intermediate (SI Figure 6).

The first experiment performed provided a time frame for key ^{15}N containing intermediates (Figure 3, Supplemental Video 1). For example, from the time-lapse video it can be determined that the first major intermediate (red box in Figure 3a) with correlations from the ^{15}N to protons on **7** begin appearing at two hours and disappear by 12 hours, whereas the second major intermediate (blue box in Figure 3a) appears at 4 hours and disappears at 14 hours. From this timeline, we carried out additional 2D NMR experiments, such as ^{1}H – ^{1}H COSY, ^{1}H – ^{13}C HSQC, and ^{1}H-^{13}C HMBC to elucidate the structural identity of the time sensitive intermediates (Figure 3b).

The starting material ^{15}N-anthranilic acid has a ^{15}N shift of δ -311.1 ppm and a strong correlation to aromatic protons at δ 6.71 and 7.67 ppm. Immediately after the three reagents were added to the NMR in DMSO-d_6 we saw ^{1}H-^{15}N HMBC correlations from a ^{15}N shift of δ -225.0 ppm to protons at δ 6.96, 2.17, and 2.38 ppm appear, suggesting bond formation between **7** and **5**. This was validated by further COSY and HSQC correlations that established the ^{1}H's at δ 2.17 and 2.38 ppm to be the methylene of the isobutyl side-chain of the discoipyrroles. The key COSY correlations were δ 2.17 and 2.38 ppm to a septet at δ 1.28 ppm that was further coupled to methyl doublets at δ 0.62 and 0.70 ppm. The slightly downfield chemical shift of the diastereotopic methylene and the ^{15}N chemical shift indicated an electron withdrawing environment, potentially suggesting a pyrrole ring. This was confirmed by ^{1}H-^{13}C HMBC correlations from methylene protons to carbons at δ 127.0 and 138.5 ppm consistent with structure of **I**. The absence of ^{1}H-^{13}C HMBC correlations between these carbons and exchangeable NH ^{1}H signals further suggested the formation of the pyrrole ring.

A weaker ^{15}N signal of δ -254.9 ppm appeared with correlations to an aromatic proton at δ 6.95 ppm and aliphatic signals at δ 4.40 and 1.34 ppm. Using similar strategies as described for **I**, correlations between these signals and to the isobutyl chain led to structure **II**, the ketone tautomer of **I**.

After 16 hours, the ^{1}H-^{15}N HMBC correlations of **I** and **II** decrease, while a third ^{15}N signal at δ -248.3 ppm appears with correlations to protons at δ 7.24 and 1.69 ppm, representing compound **III**. Up to 24 hours into the reaction, this signal existed independently and continued to build in intensity. Due to the apparent stability and abundance of the intermediate an aliquot of the reaction was removed and subjected to LC/MS analysis. The retention time and mass indicated that compound **III** was the open form of discoipyrrole that exists in pH dependent equilibrium with **1**. This reaction was repeated at a later time to yield larger quantities of **III**, which was isolated and characterized in full (SI Table I).

After 24 hours, 1% TFA was added to the NMR tube and monitoring via ^{1}H-^{15}N HMBC was continued. In the first NMR scan after acid addition, two ^{15}N species at δ -251.3

ppm, with ^{1}H correlations to δ 7.29 and 1.67 ppm, and δ -246.4 ppm, with proton correlations to δ 7.61, 1.75, and 1.44 ppm, appeared. Within minutes, a major ^{15}N species of δ -263.8 ppm with correlations to ^{1}H of δ 6.29, 2.06, and 1.91 ppm appeared. This was assigned as the final product, **IV**.

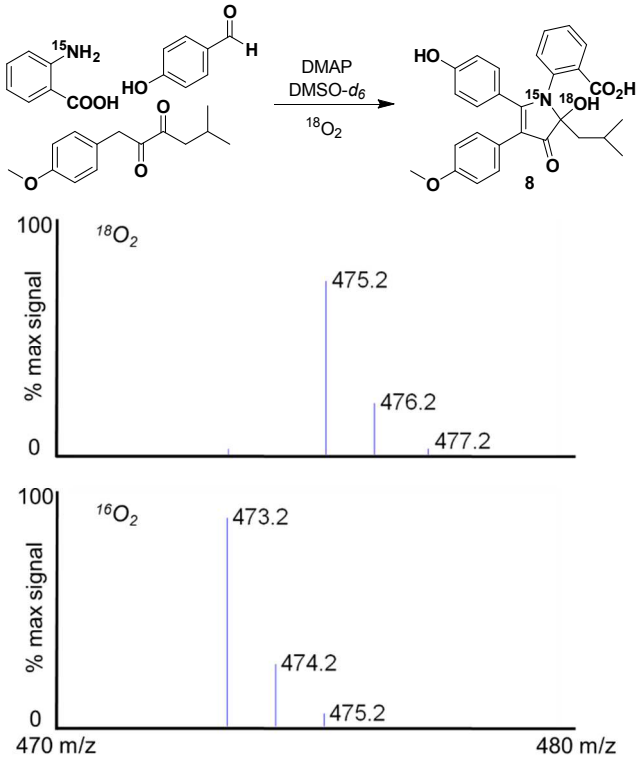

Figure 4. Formation of discoipyrrole analog **8** under an atmosphere of $^{18}O_2$. $[M - H]^-$ data confirming incorporation of ^{18}O with representative control experiment carried out with $^{16}O_2$.

These experiments demonstrated that the formation of the pyrrole core of the discoipyrroles occurs rapidly to produce the first major intermediate, **I**, which persists in equilibrium with the tautomer **II**. The loss of oxygen indicated that formation of the C-N bond in **I** induces an elimination of water. Subsequent oxidation of the pyrrolone ring to yield **III**, which under exposure to acid undergoes cyclization to **IV**. It should be noted that it is also possible that **I** is directly oxidized to **III** and that we only observe **II** as part of the equilibrium with **I**. To confirm this mechanism, we carried out the formation of **III** identical conditions under an atmosphere of $^{18}O_2$. Monitoring of the reaction by LC-MS led to observation of a peak with an *m/z* $[M - H]^-$ of 475.2, a +2 shift from canonical **III** as evident by the control reaction run with $^{16}O_2$ (Figure 4). Acid free isolation and high resolution mass spectrometry of the ^{18}O-labeled product gave an experimental value of an *m/z* $[M + H]^+$ of 477.1923 (expected $[M + H]^+$ *m/z* = 477.1924). The isolated ^{16}O control product gave an experimental value *m/z* $[M + H]^+$ of 475.1881 (expected $[M + H]^+$ *m/z* = 475.1881) (SI Figure 7-8). This unusual oxidation of the pyrrole moiety is unaffected by substitution of either the substitutents on the benzaldehyde or anthranilic acid moeities.

Isolation of the ^{18}O-labeled analog of **III** allowed us to explore the acid-induced ring closure. Surprisingly, exposure to TFA led to an isolated product with *m/z* $[M + H]^+$ of 457.1774 (expected $[M + H]^+$ *m/z* = 457.1776) that indicated the loss of ^{18}O label upon ring closure (SI Figure 9). This suggests under these anhydrous, acidic conditions that the elimination of H_2O leads to imine formation, followed by rapid cyclization.

While monitoring ^{1}H-^{15}N HMBC, we could detect no intermediates prior to pyrrole formation, i.e. no combination of **5** with either **7** or with **6** alone. This indicated to us that formation of intermediate **I** was irreversible and the multicomponent reaction occurred too rapidly to be detected by isotope enhanced NMR. We hypothesized that there were three potential pathways to form **I** (Figure 5, *pathways 1 – 3*). To test these individually, we performed three independent reactions, each with one of the substrates omitted. These reactions were performed using the described model conditions, except when noted.

Pathway 1 relies on initial formation of an aldimine between **5** and **6**, setting up for a Mannich reaction. We monitored for imine formation using ^{1}H–^{15}N HMBC with an expected imine ^{15}N shift in the 0 – 100 ppm range. Under model conditions, after 24 hours there was no formation of **9 (**Figure 6). This was further confirmed by LC-MS analysis. As a control reaction we were readily able to form aldimine **10** between ^{15}N aniline and **6** under the model conditions to give a product with a ^{15}N δ at -65.0 ppm (Figure 6). This suggests that the mechanism of discoipyrrole formation does not go through a Mannich reaction. To further test this, we took commercially available **9, 7** and DMAP in our model conditions and monitored for formation of **III** by LC-MS. Product was not detected after 48 hours, well within the timeframe expected for product formation to occur.

To test pathway 2, [1-^{13}C]-**6** and **7** were treated with DMAP and monitored by NMR and LC-MS looking for the Claisen-Schmidt product. After 48 hours we only observed the presence of [1-^{13}C]-**6** and **7**. Increasing reaction time, temperature, or strength of the base did not facilitate any condensation. It is possible that anthranilic acid could act as a catalyst for the Claisen-Schmidt reaction, however the complete lack of product formation under all of the conditions attempted is strong evidence against pathway 2.

Pathway 3, in which **7** undergoes imine formation was tested by omitting **6** in the reaction. However to our surprise, after 24 hours the main product was a dimethoxy discoipyrrole analog. Utilizing NMR and LC/MS we observed 4-methoxybenzaldehyde in the reaction, demonstrating that **7** could be degraded to form 4-methoxybenzaldehyde. Therefore, aldehyde contamination of reactions involving oxidized sattabacin analogs prevented further analysis due to the shuttling of intermediates to pyrrole formation.

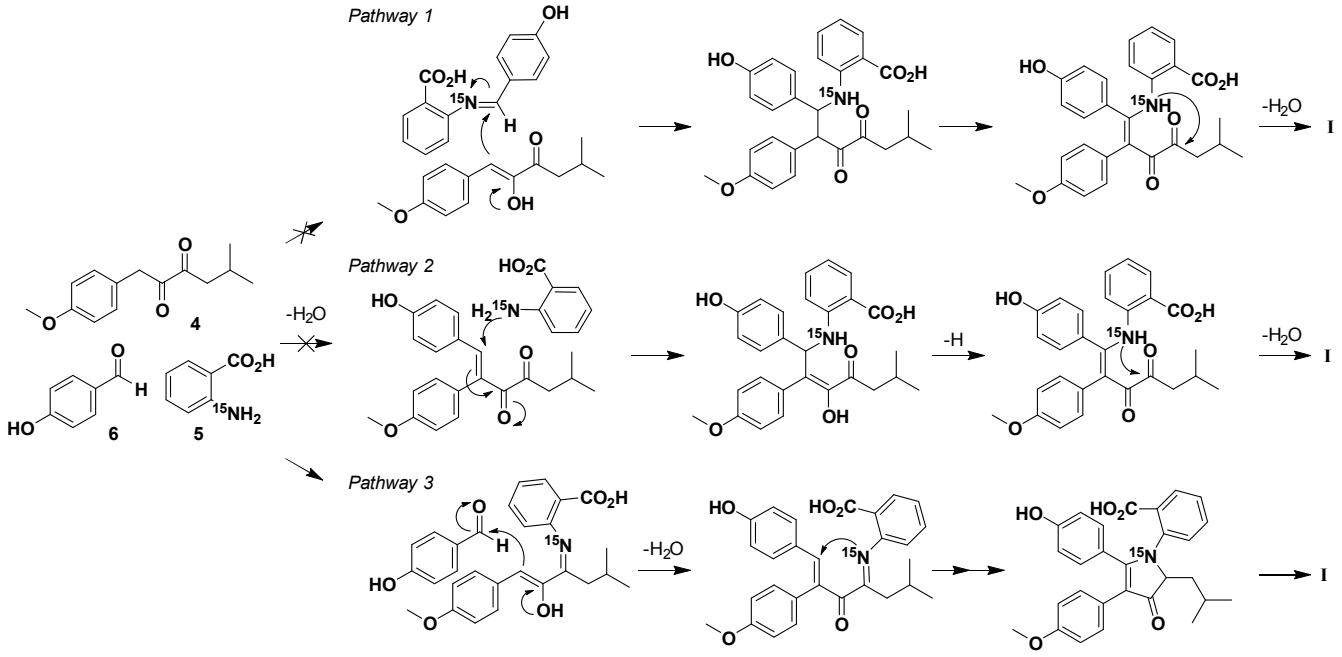

Figure 5. Possible pathways to pyrrole core intermediate **I**.

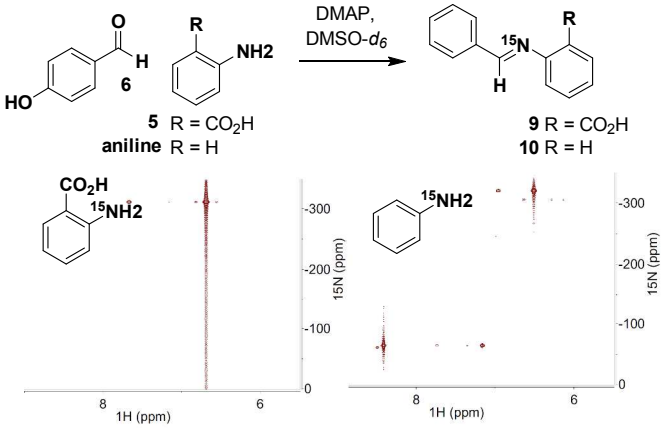

Figure 6. Using ^{1}H-^{15}N HMBC to monitor formation of aldimine between **6** and aniline and **6** and **5**.

To circumvent this issue, we utilized 4-hydroxysattabacin in lieu of **7**, removing the possibility for condensation with aldehyde coming from **7**. No discernable amount of the desired product was detected, however slightly increased temperatures induced minor product formation. We reasoned that an equilibrium between the acyloin group and any imine might favor the former, compared to the diketone of **7**. Therefore, we set out to trap potential amination products using reductive conditions. Indeed, reacting 4-hydroxysattabacin and anthranilate in the presence of sodium triacetoxyborohydride in dichloroethane with acetic acid yielded a reductive amination product (31% yield) within 16 hours (SI Figure 10). Reduction of 4-hydroxysattabacin to the diol side product was prevalent, potentially obscuring the calculated reaction efficiency.

The efficiency of these omission experiments compared to the complete reaction containing all three reactants indicated that the mechanism was enhanced by a concerted flow of reactivity. Our current hypothesis is that pyrrole formation can proceed through amination of **7** by anthranilic acid to an imine intermediate that can be trapped by a Claisen-Schmidt condensation between the C1 position of sattabacin and 4-hydroxybenzaldehyde. We believe that the amination increases the acidity of the C1 methylene to cause the "snapping" together of the three substituents. The resulting conjugated olefin can then be attacked by the nitrogen of anthranilic acid to form the five membered core.

CONCLUSION

The discoipyrroles presented a unique biosynthetic case, in that they can be produced by a specific and concerted mechanism in aqueous media from diverse excreted metabolites. To study how anthranilic acid, 4-hydroxybenzadehyde, and 4-hydroxysattabacin were able to undergo such a reaction we constructed a model system in organic solvent and utilized various analytical techniques, including the novel application of ^{1}H-^{15}N HMBC as a tool for monitoring reactions *in situ*. Building on the foundation made possible by this technique, we performed various isotope labeling experiments with ^{13}C, ^{15}N, and ^{18}O to elucidate the mechanism of non-enzymatic discoipyrrole formation. This multi-component reaction was characterized by the initial, rapid steps to induce pyrrole formation and the following changes in oxidation state that dictate the final closure of the lactone ring. Particularly useful was the ^{18}O labeling experiments which allowed us to clearly demonstrate the atmospheric oxidation of the pyrrolone using careful isolation and high resolution mass spectrometry. Furthermore, the subsequent loss of this isotope was integral in establishing the dehydration dependent lactone ring closure.

Importantly, once the details of the mechanism were uncovered, we constructed fermentation media with deuterated water and used our ^{1}H-^{15}N HMBC monitoring method to validate discoipyrrole formation in biologically equivalent conditions without organic solvent or added DMAP (SI Figure 11). We observe identical intermediates and a similar reaction time course under both conditions.

Aryl amines are found to participate in many of the recent examples of natural products amenable to non-enzymatic incorporation including the ammosamides, elansolids, and oxazinin A[5-6]. Through our mechanistic studies of the DPs, we

have shown that anthranilic acid acts as the initiating factor through imine formation with sattabacin and that the *ortho* carboxylic acid substitution of anthranilate drives the selectivity as seen in the aldimine formation experiments (Figure 6). Our work and others suggest that aryl amines play a significant role in non-enzymatic reactions and that aryl substitution patterns, the nature of the amination sites, and the stability of intermediates all contribute to the complexity of these reactions. Using these types of nucleophiles could be a potentially cost effective and simple way to screen bacterial libraries for natural products amenable to non-enzymatic perturbations. Concordantly, detection methods using ^{15}N labels such as the ^{1}H-^{15}N HMBC demonstrated here could provide quick and high sensitivity analysis.

ASSOCIATED CONTENT

Supporting Information

General procedures, data tables, NMR spectra, and additional data are described. This material is available free of charge via the Internet at http://pubs.acs.org.

AUTHOR INFORMATION

Corresponding Author

* john.macmillan@utsouthwestern.edu

Notes

The authors declare no competing financial interest.

ACKNOWLEDGMENT

We acknowledge Jonathan R. Goodman and Dr. Wade C. Winkler (University of Maryland) for their gracious contribution in the sequencing and processing of the *Bacillus hunanensis SNA-048* genome. We acknowledge following grants for funding this project: Welch Foundation I-1689 and NIH R01CA1499833, NIH U01CA176284, the Chilton/Bell Foundation and the Martha Steiner family.

REFERENCES

(1) Hu, Y.; Potts, M. B.; Colosimo, D.; Herrera-Herrera, M. L.; Legako, A. G.; Yousufuddin, M.; White, M. A.; MacMillan, J. B. *J. Am. Chem. Soc.* **2013,** *135*, 13387-92.

(2) Shih, J. L.; Nguyen, T. S.; May, J. A. *Angew. Chem., Int. Ed. Engl.* **2015,** *54*, 9931-5.

(3) (a) Clardy, J.; Walsh, C. *Nature* **2004,** *432*, 829-837; (b) Fischbach, M. A.; Walsh, C. T. *Chem. Rev.* **2006,** *106*, 3468-3496.

(4) (a) Cottreau, K. M.; Spencer, C.; Wentzell, J. R.; Graham, C. L.; Borissow, C. N.; Jakeman, D. L.; McFarland, S. A. *Org. Lett.* **2010,** *12*, 1172-5; (b) Zhu, X.; Liu, J.; Zhang, W. *Nat. Chem. Biol.* **2015,** *11*, 115-120; (c) Asai, T.; Tsukada, K.; Ise, S.; Shirata, N.; Hashimoto, M.; Fujii, I.; Gomi, K.; Nakagawara, K.; Kodama, E. N.; Oshima, Y. *Nat. Chem.* **2015,** *7*, 737-743.

(5) Pan, E.; Oswald, N. W.; Legako, A. G.; Life, J. M.; Posner, B. A.; Macmillan, J. B. *Chem. Sci.* **2013,** *4*, 482-488.

(6) (a) Lin, Z.; Koch, M.; Abdel Aziz, M. H.; Galindo-Murillo, R.; Tianero, M. D.; Cheatham, T. E.; Barrows, L. R.; Reilly, C. A.; Schmidt, E. W. *Org. Lett.* **2014,** *16*, 4774-4777; (b) Steinmetz, H.; Gerth, K.; Jansen, R.; Schläger, N.; Dehn, R.; Reinecke, S.; Kirschning, A.; Müller, R. *Angew. Chem. Int. Ed.* **2011,** *50*, 532-536; (c) Steinmetz, H.; Zander, W.; Shushni, M. A. M.; Jansen, R.; Gerth, K.; Dehn, R.; Dräger, G.; Kirschning, A.; Müller, R. *ChemBioChem* **2012,** *13*, 1813-1817.

(7) (a) Kanehisa, M.; Goto, S. *Nuc. Acids Res.* **2000,** *28*, 27-30; (b) Kanehisa, M.; Goto, S.; Sato, Y.; Kawashima, M.; Furumichi, M.; Tanabe, M. *Nuc. Acids Res.* **2014,** *42*, D199-205.

(8) (a) Park, J. S.; Kagaya, N.; Hashimoto, J.; Izumikawa, M.; Yabe, S.; Shin-Ya, K.; Nishiyama, M.; Kuzuyama, T. *ChemBioChem* **2014,** *15*, 527-32; (b) Balskus, E. P.; Walsh, C. T. *J. Am. Chem. Soc.* **2008,** *130*, 15260-1; (c) Gocke, D.; Nguyen, C. L.; Pohl, M.; Stillger, T.; Walter, L.; Müller, M. *Adv. Syn. Cat.* **2007,** *349*, 1425-1435.

(9) (a) Cleland, W. W. *Arch. Biochem. Biophys.* **2005,** *433*, 2-12; (b) Gomez-Gallego, M.; Sierra, M. A. *Chem. Rev.* **2011,** *111*, 4857-963.

(10) (a) Mahmud, T. *J. Labelled Comp. Radiopharm.* **2007,** *50*, 1039-1051; (b) Esquenazi, E.; Jones, A. C.; Byrum, T.; Dorrestein, P. C.; Gerwick, W. H. *Proc. Natl. Acad. Sci. U S A* **2011,** *108*, 5226-31; (c) Rinkel, J.; Dickschat, J. S. *Beilstein J. Org. Chem.* **2015,** *11*, 2493-2508.

(11) (a) Vizcaino, M. I.; Crawford, J. M. *Nat. Chem.* **2015,** *7*, 411-7; (b) Bode, H. B.; Reimer, D.; Fuchs, S. W.; Kirchner, F.; Dauth, C.; Kegler, C.; Lorenzen, W.; Brachmann, A. O.; Grun, P. *Chemistry* **2012,** *18*, 2342-8; (c) Kwon, Y.; Park, S.; Shin, J.; Oh, D. C. *Arch. Pharm. Res.* **2014,** *37*, 967-71.

For Table of Contents Only

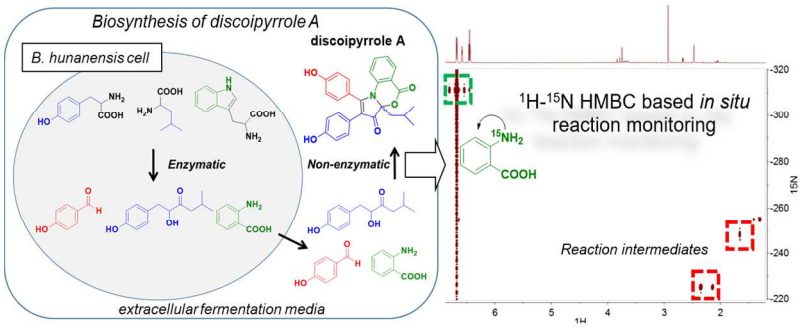
Biosynthesis of discoipyrrole A
B. hunanensis cell
discoipyrrole A
Enzymatic
Non-enzymatic
extracellular fermentation media
^{1}H-^{15}N HMBC based *in situ* reaction monitoring
Reaction intermediates